T_{12c} may be expressed as

$$T_{12c} = t_{12c1} + t_{12c3} + t_{12c5} + t_{12c7} + \cdots \tag{12d}$$

where

$$t_{12c1} = \frac{p}{2} \cdot \frac{3}{2\omega_r} \cdot \left[(e_{13} - e_{11}) \frac{b_1 - e_1}{z_1} \cos\phi_1 \right]$$
$$t_{12c3} = \frac{p}{2} \cdot \frac{3}{2\omega_r} \cdot \left[(e_{15} - e_9) \frac{b_3 - e_3}{z_3} \cos\phi_3 \right]$$
$$t_{12c5} = \frac{p}{2} \cdot \frac{3}{2\omega_r} \cdot \left[(-e_7) \frac{b_5 - e_5}{z_5} \cos\phi_5 \right]$$
$$t_{12c7} = \frac{p}{2} \cdot \frac{3}{2\omega_r} \cdot \left[(-e_5) \frac{b_7 - e_7}{z_7} \cos\phi_7 \right].$$

T_{12s} may be expressed as

$$T_{12s} = t_{12s1} + t_{12s3} + t_{12s5} + t_{12s7} + \cdots \tag{12e}$$

where

$$t_{12s1} = \frac{p}{2} \cdot \frac{3}{2\omega_r} \cdot \left[-(e_{11} + e_{13}) \frac{b_1 - e_1}{z_1} \sin\phi_1 \right]$$
$$t_{12s3} = \frac{p}{2} \cdot \frac{3}{2\omega_r} \cdot \left[-(e_9 + e_{15}) \frac{b_3 - e_3}{z_3} \sin\phi_3 \right]$$
$$t_{12s5} = \frac{p}{2} \cdot \frac{3}{2\omega_r} \cdot \left[(-e_7) \frac{b_5 - e_5}{z_5} \sin\phi_5 \right]$$
$$t_{12s7} = \frac{p}{2} \cdot \frac{3}{2\omega_r} \cdot \left[(-e_5) \frac{b_7 - e_7}{z_7} \sin\phi_7 \right].$$

REFERENCES

[1] P. Pillay and R. Krishnan, "Modeling, simulation, and analysis of permanent-magnet motor drives, Part I: The permanent-magnet synchronous motor drive," *IEEE Trans. Ind. Applicat.*, vol. 25, pp. 265–273, Mar./Apr. 1989.

[2] P. Pillay and R. Krishnan, "Modeling, simulation and analysis of permanent-magnet motor drives, Part II: The brushless DC motor drive," *IEEE Trans. Ind. Applicat.*, vol. 25, pp. 274–279, Mar./Apr. 1989.

[3] T. M. Jahns, "Torque production in permanent-magnet synchronous motor drive with rectangle current excitation," *IEEE Trans. Ind. Applicat.*, vol. IA-20, pp. 803–813, July/Aug. 1984.

[4] H. R. Bolton and R. A. Ashen, "Influence of motor design and feed-current waveform on torque ripple in brushless DC drives," *Proc. Inst. Elect. Eng.*, vol. 131, pt. B, no. 3, May 1984.

[5] H. Le-Huy, R. Perret, and R. Feuillet, "Minimization of torque ripple in brushless DC motor drives," *IEEE Trans. Ind. Applicat.*, vol. 22, pp. 748–755, July/Aug. 1986.

[6] J. Y. Hung, "Design of the most efficient excitation for a class of electric motor," *IEEE Trans. Circuits Syst.*, vol. 41, pp. 341–344, Apr. 1994.

[7] D. C. Hanselman, "Minimum torque ripple, maximum efficiency excitation of brushless permanent magnet motors," *IEEE Trans. Ind. Electron.*, vol. 41, pp. 292–300, June 1994.

[8] P. Pillay and R. Krishnan, "An investigation into the torque behavior of a brushless DC motor," in *Proc. IEEE-IAS Annu. Meeting*, 1988, pp. 201–208.

A Trajectory Feedback Control for the Computer Disk File Track-Accessing/Following Servo

Jia-Yush Yen and So-Zen Tsai

***Abstract*—This letter presents the idea of using the distances along the time-optimal state trajectory for the feedback parameters in the computer disk file servo. The method allows smooth switching between saturated control efforts and can eliminate the common overshoot problem. Due to the nature of the feedback information, the method achieves both track accessing and track following with a single stage of control.**

***Index Terms*—Disk drive servo, saturated control, trajectory feedback.**

I. INTRODUCTION

This letter presents the idea of using the distance along the time-optimal state trajectory as the feedback parameter in the computer hard disk servo system. The modern computer disk drives use bang-bang-type track-accessing controllers to move the data head from one track to another. Separate track-following controllers will then keep the head over the prespecified tracks [1]. Several problems are associated with this mechanism [2]. First of all, there is always a limit on the maximum allowable speed to avoid excessive jerk on the slider. Secondly, the state mismatch during the transition between the accessing and the following servos often leads to undesirable track overshoot. Thirdly, a large amount of deceleration force must be reserved to further slow down the slider when its speed exceeds the preset speed limit. As a result, the deceleration curve is much more flattened than the acceleration curve, and the deceleration phase takes a much longer time. It is important in the disk drive servo practice not to allow the head to move across the maximum deceleration curve. Once the head moves over the maximum deceleration curve, there will not be enough force to pull it back to the normal trajectory. This will result in highly oscillatory settling and make control very difficult [3].

In this letter, the trajectory feedback controller (TFC) introduced in [4] is extended to the disk drive servo application. The proposed algorithm is a near time-optimal control which uses the remaining distance to the switching surface as the feedback parameter. The controller maintains a time margin by using the feedback information and, thus, requires no reserved effort. The simulation result on a Zentek SCANPI disk drive model shows better accessing time characteristics than the traditional reference profile method.

II. TRAJECTORY FEEDBACK FOR THE COMPUTER DISK DRIVE SERVO

Referring to Fig. 1, the TFC uses the distance along the optimal state trajectory s_i to the next switching curve as the feedback information [4]:

$$s_i = \mathrm{sgn(u)} \int_{\mathrm{p_i}-1}^{\mathrm{p_i}} \mathrm{d\bar{s}}, \quad \mathrm{i} = 1, 2, \cdots \tag{1}$$

where p_{i-1} is the position of the current state after the ith switching of control effort and p_i is the location of the next switching point in the state-space portrait.

Manuscript received May 24, 1996; revised April 22, 1997.

The authors are with the Department of Mechanical Engineering, National Taiwan University, Taipei 10764, Taiwan, R.O.C. (e-mail: jyen@ccms.ntu.edu.tw).

Publisher Item Identifier S 0278-0046(97)06517-9.

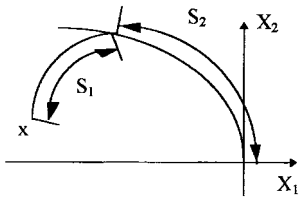

Fig. 1. The trajectory feedback control.

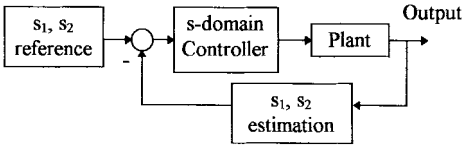

Fig. 2. Trajectory feedback compensator.

Consider the second-order pure inertia model used in track accessing; the feedback parameters are the distances s_1 and s_2 shown in Fig. 1. For this model, their values can be evaluated by

$$s_1 = \frac{1}{4JU}\left[2U^2\sinh^{-1}\left(\frac{\sqrt{2J(Jv^2-2pU)}}{2U}\right) + \sqrt{J(Jv^2-2pU)(J^2v^2+2U^2-2JpU)}\right] - \frac{1}{2JU}\left[U^2\sinh^{-2}\left(\frac{Jv}{U}\right)+Jv\sqrt{J^2v^2+U^2}\right] \quad (2)$$

$$s_2 = \frac{U}{2J}\sinh^{-1}\left(\frac{J\sqrt{2J(Jv^2-2pU)}}{2U}\right) + \frac{1}{4U}\sqrt{\left(v^2-\frac{2pU}{J}\right)(J^2v^2+2U^2-2JpU)} \quad (3)$$

where J is the system inertia, U is the maximum input effort, $p = x_1$ is the current position, and $v = x_2$ is the current velocity. With the s-parameter feedback, the control algorithm becomes as shown in Fig. 2, and the control effort is basically $u_i = U_{\max}\mathrm{sgn(s_i)}$, where "sgn" is the sign of s_i. During the control process, the s_2 parameter is first kept constant as the s_1 parameter reduces. Since the control uses full actuation force while s_2 is kept constant, the plant will move along a parallel trajectory to the optimal trajectory to reach the switching curve. After s_1 has reduced to (or come close to) zero, the s_2 control will switch on, and the control action will change to reduce the s_2 parameter and move the state toward the origin along the optimal trajectory.

A. Avoiding Overshoot

One can view the control action as suppressing the degree of freedom of the system state. The s_1 and s_2 parameters are measures of the "sizes" of the subspaces that are being suppressed. From (2) and (3), when the s_1 parameter crosses zero, the second stage of control becomes a new first stage, and the trajectory along the new path becomes s_1. Thus, s_1 serves as a good indicator for overshooting beyond the switching curve. Using this property, a deadband is introduced to s_1 to avoid overshoot:

$$s_1 = \begin{cases} \int_{nT}^{(n+1)T}\left|\frac{d\vec{R}}{dt}\right|dt, & \text{for } n \geq 0, n \in Z \\ 0, & \text{for } 0 \leq n < 1 \end{cases} \quad (4)$$

where $\vec{R}$ stands for the position vector of the state in the phase portrait, n is the sampling instance before s_1 crosses the switching curve, Z stands for integer, and T is the sampling interval. When s_1 is set to zero, the TFC will switch to the s_2 control, and the system will start to move parallel to the deceleration trajectory, thus preventing the state from moving across the switching curve.

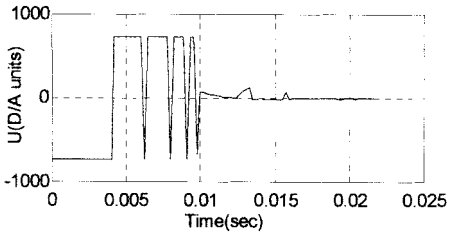

(a)

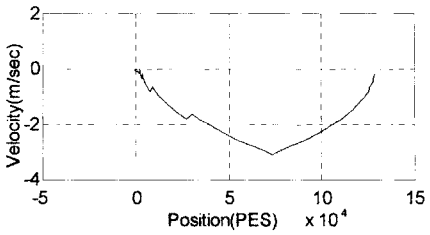

(b)

Fig. 3. Simulation results using TFC. (One PES is equivalent to 0.054 μm, one control unit u generates 0.021 N·m of control torque.) (a) The control input. (b) The $X1$–$X2$ plane.

B. Suppressing Chattering

The s-domain control with (4) does not prevent the system from chattering; however, due to the nature of the TFC control, $u = U_{\max}\mathrm{sgn(s_i)}$, it is possible to introduce a scaling factor to the control effort as s_i approaches zero to suppress the chattering. For the second-order system model in this letter, the control would become $u = \alpha U_{\max}\mathrm{sgn(s_2)}$. Note that $s_2 = f(x_1, x_2, \cdots)$. When s_2 is small, the control effort can be approximated by $u = k_1x_1 + k_2x_2$. For practical applications, the k_i's can be selected to be a high-performance state feedback gain. Thus, the switching only occurs in the feedback gains, and the problem of state mismatch no longer exists. The control algorithm at this stage is equivalent to a high-performance state feedback control around the origin and, thus, possesses the robustness property offered by state feedback.

III. Simulation Results

The simulation is based on the Zentek Scanpi disk drive model. The sampling rate is 4.5 kHz. There are 0–1560 tracks on the disk. Track density is 1850 TPI, therefore, the track width is 13.73 μm. The position error signal (PES) for each track is divided into 256 levels from the A/D converter, thus, the sensor resolution is 0.054 μm. The effective inertia is $J = 3.48 \times 10^{-4}$ kg·m^2, and the maximum voice coil input signal is $|U| = 728$, equivalent to a control torque of 15.4 N·m. Fig. 3 shows the responses for a 500-track seek. It is worth noting that, for practical implementation, it is very difficult for the hardware to handle the s-domain calculation. Fortunately, this part of the calculation can be done beforehand, using a lookup table in the application. From Fig. 3, one can clearly see the saturated control for the accessing process. As the trajectory enters the final zone, the system smoothly transfers to state feedback track-following control.

IV. Conclusion

The trajectory feedback control has been extended for use in the computer disk file actuator servo. The method allows

smooth transition between saturated efforts. It avoids overshoots in the phase portrait and also suppresses chattering. As the system comes close to the origin, the control converges to a state feedback control. Therefore, the method enables a smooth transition from accessing into following control within the same control algorithm and maintains the robustness property of the state feedback controller. The simulation results confirm a saturated control during the accessing process and a smooth transition into high bandwidth track following as the head comes close to the target track.

REFERENCES

[1] M. L. Workman, R. L. Kosut, and G. F. Franklin, "Adaptive proximate time optimal control: Continuous time case," in *Proc. Automatic Control Conf.*, 1987, pp. 589–594.

[2] C. D. Mee and E. D. Daniel, *Magnetic Recording Handbook: Technology and Applications*. New York: McGraw-Hill, 1990.

[3] R. D. Commander and J. R. Taylor, "Servo design for an eight-inch disk file," *IBM Disk Storage Technol.*, pp. 90–98, Feb. 1980.

[4] T.-Y. Hwang, J.-Y. Yen, and S.-S Lu, "Bang-bang based fuzzy controller for time optimal and minimum chattering servo systems," *Elec. Mach. Power Syst.*, vol. 23, no. 1, pp. 25–35, Jan. 1995.